

The shock and release behaviour of an aerospace-grade cured aromatic amine epoxy resin

PJ Hazell, C Stennett and G Cooper

Dynamic Response Group, Department of Materials and Applied Science, Cranfield University, Defence College of Management and Technology, Shrivenham, SN6 8LA, UK

ABSTRACT

Knowing the dynamic behaviour of polymer materials that are used in the construction of fibre reinforced composite materials is particularly important for such materials that are subjected to impact. In this work, we have conducted a number of plate impact experiments on a commercially important aromatic amine epoxy resin that is used in the construction of carbon fibre composite materials. The measured Hugoniot in shock velocity – particle velocity space is $U_s = 2.65 + 1.55u_p$ ($\rho_0 = 1.141$ g/cc) and is similar to the measured Hugoniot of other resins presented by different researchers. We have also measured the longitudinal stress in the shocked material and shown, in common with other polymers, that above a threshold stress, an increase in shear stress behind the shock wave is observed.

I. INTRODUCTION

Understanding the dynamic response of polymer materials is becoming increasingly important due to their use in explosive compositions, warhead design and composite material construction. For the latter example, glass fibre reinforced composite laminates have been used for many years in armour systems that are inherently subjected to shock [1]. The shock response of carbon fibre / epoxy composites is also of interest due to these materials becoming more commonly used in military and civilian aircraft. Consequently the response of these materials due to high velocity impact of small projectiles has been studied. [2-5]

An important constituent part to a carbon fibre reinforced plastic is the polymeric matrix. Carter and Marsh [6] conducted an extensive study on the shock response of polymer materials, and showed that a significant number of polymers, and indeed an epoxy resin, undergo a change in slope in the shock velocity – particle velocity curve at high stresses (~20-30GPa). The authors thought that this was probably best explained in terms of pressure-induced cross-linking of the long polymer chains. In particular, for the polymers that contained aromatic rings in their monomer structure and that showed the largest volume change at transformation, it was proposed that tetragonal bonds form between the chains in a manner analogous to the graphite / diamond transformation. Other researchers have shown that for polymers that contain a phenyl ring, such as polystyrene, this behaviour can be explained in terms of the ring's collapse at the elevated pressures [7]. Other researchers have shown that certain polymers have a positive dependence on shear strength with increasing shock stress. This behaviour has

been seen in polycarbonate [8], PMMA [9], and PTFE [10] with embedded lateral gauges. This behaviour has also been observed in the elastomer Estane™ [10].

Unlike metals, thermoplastic polymers and ceramics, there is a paucity of data dealing with the shock response of thermoset epoxy resins. This is perhaps surprising as these resins are integral to the construction of considerable civilian and military hardware that is subjected to shock. Munson and May [11] investigated three different epoxy resin systems that used different hardening agents. They found that, within experimental error, the measured Hugoniot of the material was the same for each resin. Barnes *et al* [12] have measured the Hugoniot of an epoxy resin, and found that it was very similar to that of Munson and May. Both sets of researchers assumed a linear shock velocity particle velocity relationship. Barnes *et al* suggested that, similar to the polymers mentioned above, their resin demonstrated a positive dependence of shear strength with shock stress. This positive dependence has been investigated by Bourne *et al* [13] and in accompanying work by Millett *et al* [14] who used the embedded lateral gauge technique to directly measure the variation of lateral stress. They observed that with increasing shock stress, the lateral stresses decreased resulting in an increase in strength behind the shock.

In this study, we have investigated the shock behaviour of a commercially important aromatic amine epoxy resin. This resin is a key constituent of carbon epoxy composite materials that are used by the aerospace industry. This work is part of a larger programme of work examining the impact and shock behaviour of carbon-fibre / epoxy composite materials.

II. EXPERIMENTAL TECHNIQUE

A common way for measuring the shock Hugoniot of materials is by conducting plate-impact experiments. A typical experimental set-up is shown below in Figure 1(a). Here, a flyer-plate is accelerated towards the target and arrives so that all points on the projectile's surface make contact with the target simultaneously. The impact generates a planar shock wave in the target. In this situation, all strain is accommodated along the impact axis while the orthogonal components of strain are zero due to inertial confinement.

Figure 1: (a) the Flyer plate technique, (b) schematic target assembly

The shock response of the resin target was measured using two Vishay Micro-measurements Manganin Pressure gauges LM-SS-125CH-048, encapsulated between two layers of 25 μ m Mylar. Calibration of the gauges was to Rosenberg *et al* [15]. Dural (Al 6082-T6) and copper flyers were accelerated to velocities of between 176 m/s and 992 m/s using a \varnothing 50-mm single-stage gas gun. A typical target set-up is given schematically in Figure 1(b). One gauge (the 'front-surface gauge') is fixed at the interface between the cover plate and the test specimen, and the other (the 'back surface gauge') is fixed between the test specimen and the backing material. The shock Hugoniot was measured using the standard impedance matching technique [16]. Before firing, the thickness of each test specimen was carefully measured, so that the distance between the gauges was accurately known. By measuring the time of arrival of the shock at each gauge, the (assumed constant) shock velocity (U_s) could be calculated from the transit time (Δt) of

the shock across the specimen. By knowing the Hugoniot of the flyer plate material and the impact velocity we established a value for the particle velocity (u_p) behind the shock. Hugoniot data for our flyer-plate materials were taken from Marsh [17] and the velocities of the projectile were measured by using a sequential pin shorting system to an accuracy of 0.5%. Fast digital storage oscilloscopes (2 GS/s) were used to capture the arrival and shape of the shock; subsequent data reduction and analysis was done on a PC.

III MATERIALS USED

The resin studied was a commercially available epoxy/amine resin system supplied by Hexcel Composites (Duxford UK) with the trade name RTM6. This resin was specially developed to fulfil the requirements of the aerospace composites industry in advanced resin transfer moulding (RTM) processes. It consists of a multifunctional epoxy resin cured with a mixture of aromatic amines.

The resin was fully cured at 180°C for two hours at atmospheric pressure. The resulting blocks of resin measuring 70 mm × 70 mm square and 10 mm thick were machined to 6 mm thickness and lapped to a flatness of ±5µm. The longitudinal and shear velocities were measured using 5MHz quartz transducers with a Panametrics 5077PR pulser-receiver in the pulse-echo configuration. Density was measured using a Micrometrics AccuPyc 1330 gas pycnometer. The elastic properties of the cured resin are provided in Table I.

Table I: Elastic properties of the cured RTM6 resin.

IV. RESULTS AND DISCUSSION

A typical gauge trace for the RTM6 resin is seen below in Figure 2. In this example, a 5-mm thick copper flyer was accelerated to 566 m/s prior to impact with the resin target.

Figure 2: Typical gauge trace showing the formation of the shock and release.

In each stress history, the stress rises rapidly to its maximum value in 40-50 ns. This is due to the close match between the shock impedance of the epoxy sample, the gauge backing substrate and the epoxy adhesive used to construct the gauge package. It can be seen on the front-surface gauge trace that just before the arrival of the shock there is an apparent drop in measured stress. This feature is not present on the back-surface gauge. We believe that this is due to the motion of the conducting cover plate towards the gauge, which increases the capacitance between the gauge and the cover plate. It can also be seen that there is an overshoot recorded by the front-surface gauge as the measured stress reaches its maximum value. This is due to the fast rising nature of the shock causing ringing [18]. The Hugoniot stress is measured, in this example, over the period from 0.8 to 2.2 μ s. The stress level in the back-surface gauge over the period from 2.6 to 3.6 μ s is similar to the Hugoniot stress measured by the front-surface gauge. This indicates that both the resin and the PMMA have very similar shock impedance levels.

The Hugoniot of many polymers, metals and ceramics can be fitted assuming a linear shock velocity – particle velocity relationship given by the following equation:

$$U_s = c_0 + S.u_p \quad (1)$$

where S is the slope and c_0 is the intercept of the shock velocity axis. This has previously been observed in other polymers such as PMMA [9], polycarbonate [8], polyether ether Ketone [19] and an epoxy resin [14]. For metals, c_0 has been correlated with the bulk sound speed of the material whereas S has been theoretically shown to relate to the first derivative of bulk modulus with pressure [20]. Our measured Hugoniot in shock velocity – particle velocity space is shown below in Figure 3:

Figure 3: The measured Hugoniot of the resin in shock velocity particle velocity space.

There are two points to note here. Firstly, a linear line of regression has been fitted through all ten data points resulting in c_0 and S values of 2.65 mm/ μ s and 1.55 respectively. However we note that other researchers [7,21] have shown from theoretical considerations that the Hugoniot for many polymers over a much larger particle velocity range is parabolic instead of linear. Secondly, the fitted line provides a bulk sound speed of 2.65 mm/ μ s which is higher than the ultrasonically measured value of 2.26 mm/ μ s at the frequency of the transducer (5MHz). This is consistent with epoxy behaviour, and indeed most polymer behaviour as surveyed by Carter and Marsh and points to a rapidly varying rate of change in compressibility in the low particle velocity region [6].

In Table II below we have summarised the shock parameters for epoxy resins from a number of sources. References 6, 11 and 22 used a commercially available general purpose epoxy resin Epon 828. This resin is a typical epoxy, being a condensation product of epichlorohydrin and Bisphenol-A. Millett *et al* [14] used a blend of epoxy prepolymers based on modified and unmodified Bisphenol-A, with the addition of a diglycidyl ether polypropylene glycol plasticizer. Several amine hardeners were used. Munson and May used three different hardening systems: metaphenylenediamine (MPDA); an aromatic eutectic mixture of methylenedianiline, MPDA and phenylglycidyl ether; and the organic salt of tridimethyl aminomethyl phenol. Boettger [22] used a relatively high percentage weight (30%) commercially available hardener – Jeffamine® T-403, a polyether triamine. Millet *et al* used a cycloaliphatic polyamine.

It can be seen that, despite the data being acquired by a variety of researchers over several decades for ostensibly different epoxy resin systems, the Hugoniot in shock velocity – particle velocity space are quite similar. Our data are in good agreement with those of the other researchers. This work supports the view of Munson and May, that the shock response of cured epoxy resins does not depend strongly on the degree of crosslinking, nor on the structural properties of the crosslinking chains.

Table II: Shock parameters for epoxy resin systems; the ultrasonic measurement of c_B is also added.

We have also measured the release time for each of our experiments. This was done in a systematic way by numerically differentiating the stress history, and selecting the time at

which the differential became negative. For certain experiments, there is a degree of oscillation near to the release portion of each differentiated stress history, and it is therefore difficult to obtain the precise timing of the onset of release. This uncertainty is reflected in the choice of error bars on subsequent analyses.

The distance between the two stress gauges is compressed by the passage of the shock wave according to

$$x = x_0 \left(1 - \frac{u_p}{c_0 + Su_p} \right), \quad (2)$$

where x_0 and x are the thicknesses of material before the arrival of the shock front and behind it respectively. From the compressed distance between gauges, we established the release velocity by measuring the time between releases from the shock traces.

Consequently the release wave velocity (U_R) can be calculated ($U_R = x/\Delta t_R$). This data is plotted in Figure 4.

Figure 4: A plot of the calculated release wave velocities. One data point is omitted due to premature failure of one of the gauges in that experiment.

It is interesting to note that the measured intercept (2.68 mm/ μ s) is very similar to the intercept calculated from the resin's Hugoniot (2.65 mm/ μ s). This behaviour has also been seen by Millett *et al* in polycarbonate and implies that the material returns to its ambient condition without factors such as phase transformations occurring [8]. Isbell [23]

estimates the head of the release wave to travel in metals at a velocity of $1.2U_s + u_p$ and for the RTM6 resin, this equates to a release velocity given by $U_R = 3.18 + 2.87u_p$. Given that Isbell's data are for a range of metals of varying c_0 values, including Dural, OFHC copper, Iron and Titanium it is perhaps surprising that the relationships are similar in gradient at least.

Finally, in Figure 5 below we plot the Hugoniot in longitudinal stress – particle velocity space. The gauges used in this study, and their mounting within the target, measure the longitudinal stress (σ_x) that consists of a hydrostatic component and a deviatoric component of stress in accordance with

$$\sigma_x = P + \frac{4}{3}\tau, \quad (3)$$

where P is the hydrodynamic pressure and τ is the shear stress.

Also fitted to the data is a calculation of the hydrodynamic pressure calculated by

$$P = \rho_0 U_s u_p \quad (4)$$

where U_s is calculated from Equation 1 using our experimentally determined shock parameters. Note that there is a good fit for the data at the lower particle velocities indicating that the material is behaving hydrodynamically. However beyond a shock stress of c. 4 GPa the measured stress is greater than the value predicted by the hydrodynamic curve. Similar behaviour has been observed in a range of materials from

polymers, [8,9] epoxy resins [14] and ceramics [24], and is evidence that this particular resin possesses an ability to strengthen with increasing shock stress. A possible hypothesis to explain this is that steric resistance to compression increases, as initially separate polymer chains are brought closer together and begin to interact. Other work on a range of polymers [25] has shown that the stress level at which departure from the hydrodynamic curve occurs can be modified by the choice of the side group attached to the main polymer chain. This work concluded that increasing the size of the side groups increased the resistance to compression, with polystyrene (having a phenyl side group) showing a departure from the hydrodynamic curve of c.1 GPa at 0.9 mm/ μ s. We believe that our results are consistent with this view. For the RTM6 resin, this occurs at c. 0.85 mm/ μ s.

The shock parameters from our experiments are shown in Table III.

Figure 5: Stress – particle velocity Hugoniot plots for the resin.

Table III: Experimental data.

V. CONCLUSIONS

We have measured the shock and release behaviour of a commercially important epoxy resin that is used in the manufacture of a carbon epoxy composites. The Hugoniot in shock velocity – particle velocity space is given by $U_s = 2.65 + 1.55 u_p$ ($\rho_0 = 1.141$ g/cc); the measured release wave velocity is given by $U_R = 2.68 + 3.05 u_p$. The Hugoniot is

similar in shock velocity-particle velocity space to published data for numerous resins of differing composition that has been collated over several decades. At higher shock stresses, the behaviour of the resin exhibits an increase in shear stress behind the shock wave in common with many other polymers. The specific reason for this is unclear but for other polymers this behaviour has been suggested as being due to side groups restricting compression between chains.

ACKNOWLEDGMENTS

The authors would like to thank Mr Steven Mortimer of Hexcel, Duxford, UK for supplying the cured resin samples. We also wish to thank Mrs Sally Gaulter for useful discussions. We gratefully acknowledge the UK MoD and the EPSRC who funded this work under GR/S33994/01.

REFERENCES

1. M. R. Edwards, *Comprehensive Composite Materials* 6, edited by M G Bader, K T Kedward and Y Sawada, (Elsevier Science, Oxford), p 681, (2000).
2. R. I. Hammond, W. G. Proud, H. T. Goldrein and J. E. Field. *Int J. Impact Engng.*, 30, 69 (2004).
3. K. Fujii, E. Yasuda, T. Akutsu, Y. Tanabe, *Int. J. Impact Engng.*, 28, 985 (2003).
4. V. V. Silvestrov, A. V. Plastanin, N. N. Gorshkov, *Int J. Impact Engng.* 17, 751 (1995).

5. S. Ryan, F. Schaefer and W. Riedel, *Int. J. Impact Engng.*, 33, 703 (2006).
6. W. J. Carter and S. P. Marsh, Hugoniot equation of state of polymers. LA-12006-MS, 1995.
7. D. Porter and P. J. Gould, *J. Phys. IV France*, 110, 809 (2003).
8. J. C. Millett and N. K. Bourne, *J. Mater. Sci.*, 41, 1683 (2006).
9. J. C. F. Millett and N. K. Bourne, *J. of Appl. Phys.*, 88, 7037 (2000).
10. N. K. Bourne and GT Gray III, *J. Appl. Phys.*, 98, (2005).
11. D. E. Munson and R. P. May., *J. Appl. Phys.*, 43, 962 (1972).
12. N. Barnes, N.K. Bourne and J.C.F. Millett, In *Shock Compression of Condensed Matter—2001*, edited by M.D.Furnish, N. N. Thadhani and Y. Horie, (AIP) p 135.
13. N. K. Bourne, J. C. F. Millett, N. Barnes, I Belcher, In *Shock Compression of Condensed Matter—2001*, edited by M.D.Furnish, N. N. Thadhani and Y. Horie, (AIP) p 649.
14. J. C. F. Millett, N. K. Bourne and N. R. Barnes, *J. Appl. Phys.*, 92 6590 (2002).
15. Z. Rosenberg, D. Yaziv and Y. Partom., *J. Appl. Phys.* 51, 3702 (1980).
16. L. Davison and R. A. Graham, *Physics Reports*, 55, 255 (1979).
17. S. P. Marsh, *LASL Shock Hugoniot Data*. University of California Press, Los Angeles, (1980).
18. N. K. Bourne and Z. Rosenberg, *Meas. Sci. Technol.* 8, 570, (1997).
19. J. C. F. Millett, N. K. Bourne and G. T. Gray III, *J. Phys. D: Appl. Phys.* 37, 942, (2004).
20. L. Ruoff, Linear Shock-Velocity-Particle-Velocity Relationship, *J. of Appl. Phys.* 38, 4976, (1967).

21. D. Porter and P. J. Gould, *J. Phys. IV France*, 134, 373 (2006).
22. J. C. Boettger, *SESAME Equation of State for Epoxy*, Los Alamos Report LA-12755-MS (1994).
23. W.M. Isbell, *Shock Waves: Measuring the Dynamic Response of Materials*. Imperial College Press, Singapore, ISBN 1-86094-471-X, (2005).
24. D. P. Dandekar and D. E. Grady, In *Shock Compression of Condensed Matter – 2001*, edited by M.D. Furnish, N. N. Thadhani and Y. Horie, (AIP), p 783.
25. J.C. F. Millett and N. K. Bourne, *J. Phys. D: Appl. Phys.* 37, 2901 (2004).

Table I: Elastic properties of the cured RTM6 resin.

Material	ρ_0 (g/cc)	c_L (mm/ μ s)	c_S (mm/ μ s)	c_B (mm/ μ s)	ν
RTM6	1.141 \pm 0.001	2.699	1.284	2.256	0.35

Table II: Shock parameters for epoxy resin systems; the ultrasonic measurement of c_B is also added.

Reference	ρ_0 (g/cc)	c_o (mm/ μ s)	S	c_B (mm/ μ s)
This work	1.141 \pm 0.001	2.65	1.55	2.256
Carter and Marsh [6] [†]	1.192	2.69	1.51	2.264
Munson and May [11]	1.194	2.64	1.66	2.15-2.36*
Millet <i>et al</i> [14]	1.14 \pm 0.01	2.58	1.47	1.935
Boettger [21] [†]	1.154	2.63	1.52	2.255

[†] Shock parameters for the initial slope of the $U_s - u_p$ curve taken before the apparent phase change at ~20GPa.

* Depending on the hardener.

Table III: Experimental data.

Flyer thickness material	Impact velocity (m/s)	u_p (mm/ μ s)	U_s (mm/ μ s)	U_R (mm/ μ s)	σ_x (GPa)
5 mm Al	171	0.134	2.834	3.052	0.43
5 mm Al	212	0.164	3.006	-	0.54
5 mm Cu	344	0.313	3.100	3.629	1.08
10 mm Al	460	0.360	3.300	3.910	1.34
5 mm Al	520	0.411	3.186	3.849	1.51
5 mm Cu	566	0.511	3.415	4.209	2.04
5 mm Cu	794	0.713	3.606	4.919	3.00
5 mm Cu	959	0.853	3.968	5.096	4.50
5 mm Cu	965	0.855	4.103	5.293	4.00
5 mm Cu	992	0.880	4.049	5.313	4.90

Figure 1: (a) the Flyer plate technique, (b) schematic target assembly.

Figure 2: Typical gauge trace showing the formation of the shock and release.

Figure 3: The measured Hugoniot of the resin in shock velocity particle velocity space.

Figure 4: A plot of the calculated release wave velocities. One data point is omitted due to premature failure of one of the gauges in that experiment.

Figure 5: Stress – particle velocity Hugoniot plots for the resin.

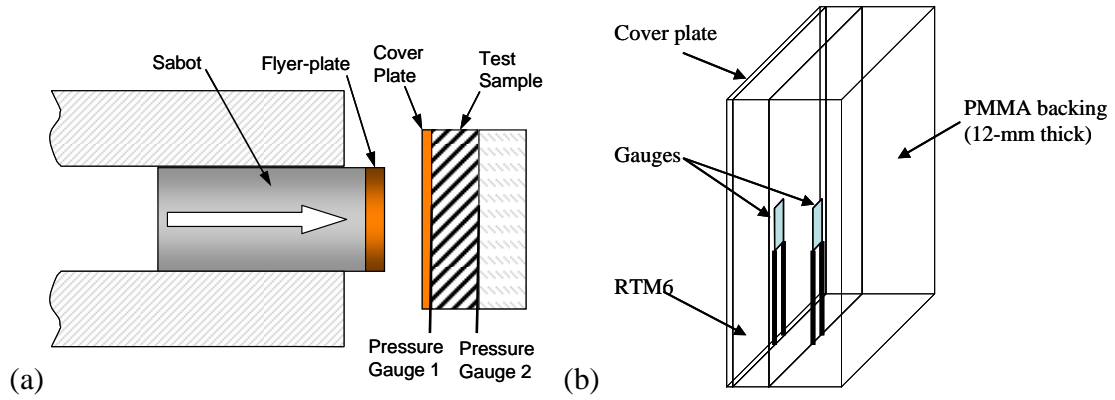


Figure 1: (a) the Flyer plate technique, (b) schematic target assembly

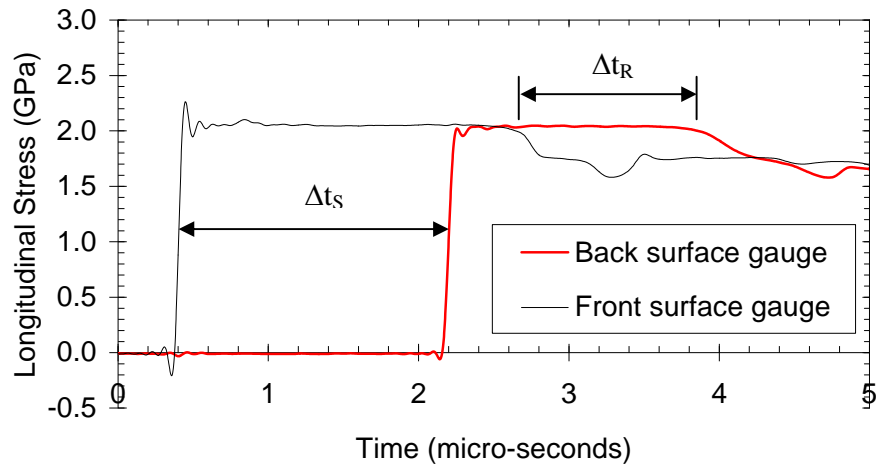


Figure 2: Typical gauge trace showing the formation of the shock and release.

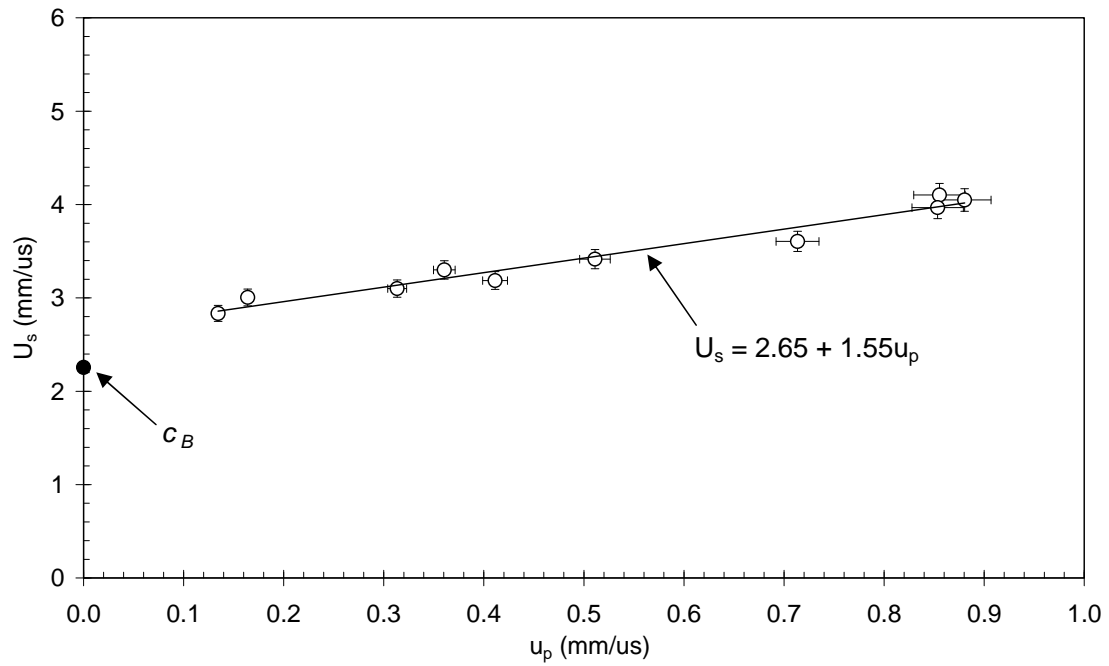


Figure 3: The measured Hugoniot of the resin in shock velocity particle velocity space.

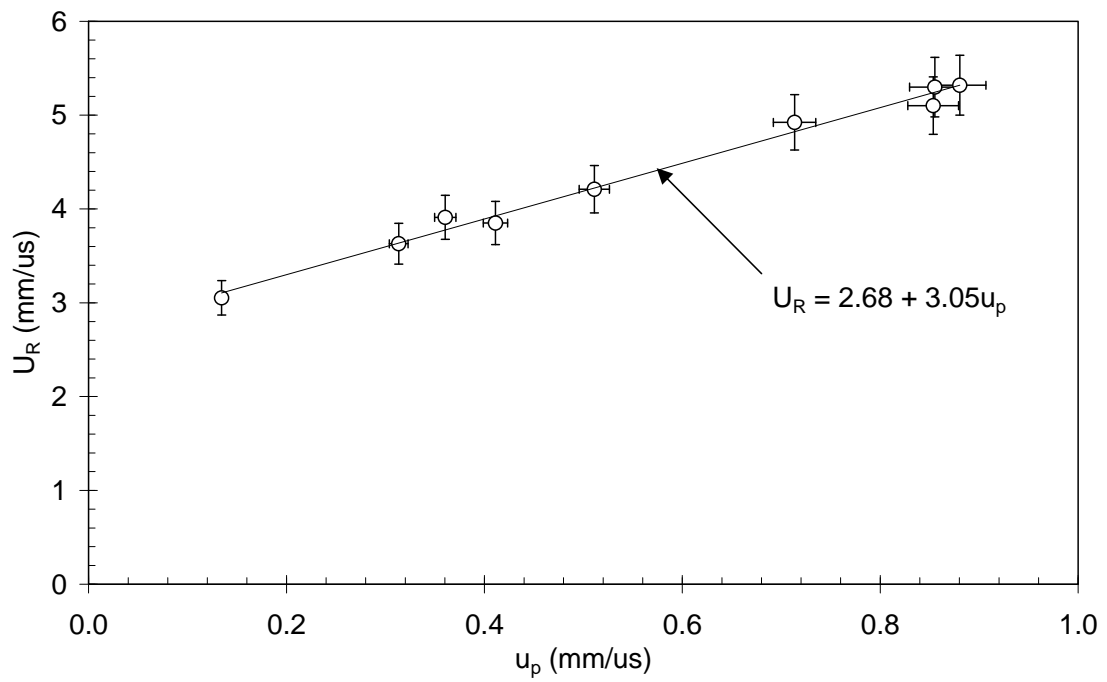


Figure 4: A plot of the calculated release wave velocities. One data point is omitted due to premature failure of one of the gauges in that experiment.

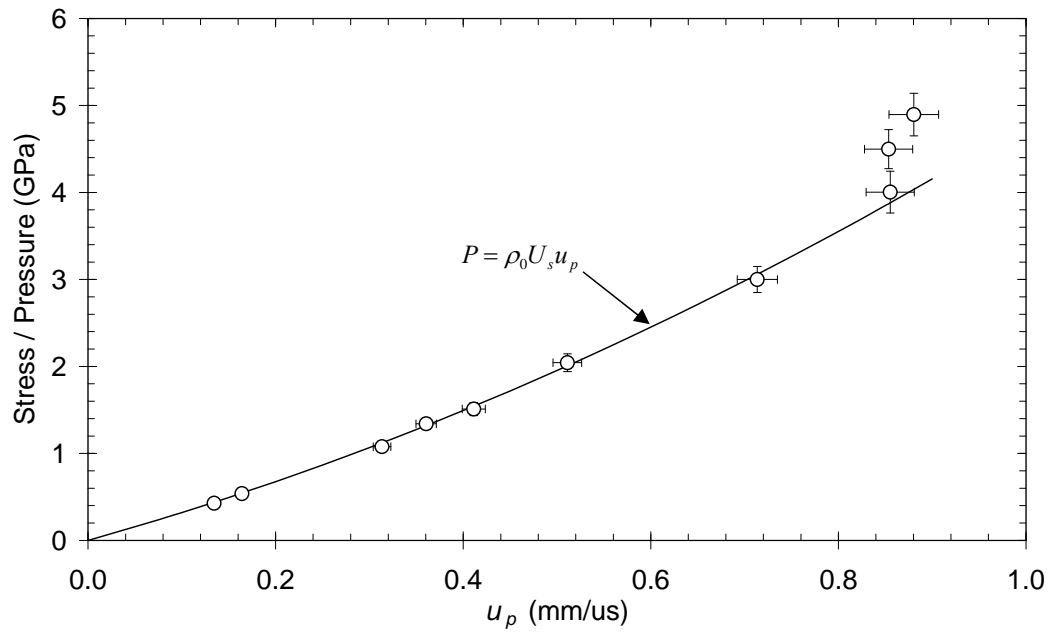


Figure 5: Stress – particle velocity Hugoniot plots for the resin.